

## Synthesis of technetium hydride $\text{TcH}_{1.3}$ at 27 GPa

Di Zhou<sup>1,\*</sup>, Dmitrii V. Semenov<sup>1,†</sup>, Mikhail A. Volkov<sup>2</sup>, Ivan A. Troyan<sup>3</sup>, Alexey Yu. Seregin<sup>3,4</sup>, Ilya V. Chepkasov<sup>1</sup>, Denis A. Sannikov<sup>1</sup>, Pavlos G. Lagoudakis<sup>1</sup>, Artem R. Oganov<sup>1</sup>, and Konstantin E. German<sup>2,‡</sup>

<sup>1</sup>Skolkovo Institute of Science and Technology, Bolshoy Boulevard 30, Building 1, Moscow 121205, Russia

<sup>2</sup>A. N. Frumkin Institute of Physical Chemistry and Electrochemistry of the Russian Academy of Sciences, Laboratory of Technetium Chemistry, Leninsky Prospekt 31-4, Moscow 119071, Russia

<sup>3</sup>Shubnikov Institute of Crystallography, Federal Scientific Research Center “Crystallography and Photonics,” Russian Academy of Sciences, 59 Leninsky Prospekt, Moscow 119333, Russia

<sup>4</sup>National Research Center “Kurchatov Institute,” Ploshchad’ Akademika Kurchatova, 1, Moscow 123182, Russia

 (Received 24 October 2022; revised 25 December 2022; accepted 5 January 2023; published 6 February 2023)

In this work, we synthesize and investigate lower technetium hydrides at pressures up to 45 GPa using synchrotron x-ray diffraction, reflectance spectroscopy, and *ab initio* calculations. In the Tc-H system, the hydrogen content in  $\text{TcH}_x$  phases increases when the pressure rises, and at 27 GPa we found a hexagonal (hcp) nonstoichiometric hydride  $\text{TcH}_{1.3}$ . The formation of technetium hydrides is also confirmed by the emergence of a reflective band at 450–600 nm in the reflectance spectra of  $\text{TcH}_{1+x}$  samples synthesized at 45 GPa. On the basis of theoretical analysis, we propose crystal structures for the phases  $\text{TcH}_{0.45\pm 0.05}$  ( $\text{Tc}_{16}\text{H}_7$ ) and  $\text{TcH}_{0.75\pm 0.05}$  ( $\text{Tc}_4\text{H}_3$ ) previously obtained at 1–2 GPa. Calculations of the electron-phonon interaction show that technetium hydrides  $\text{TcH}_{1+x}$  ( $x = 0-0.3$ ) do not possess superconducting properties due to low electron-phonon interaction parameter ( $\lambda \sim 0.23$ ).

DOI: [10.1103/PhysRevB.107.064102](https://doi.org/10.1103/PhysRevB.107.064102)

### I. INTRODUCTION

The science and technology of polyhydride materials currently have two main vectors of development: Materials for hydrogen storage and high-temperature superconductors. The first direction [1] recently received a significant boost with the discovery of pressure-stabilized polyhydrides with ultra-high hydrogen content (up to 63 wt%) such as the molecular complexes of methane  $(\text{CH}_4)_3(\text{H}_2)_{25}$  [2], hydrogen iodide  $(\text{HI})(\text{H}_2)_{13}$  [3], strontium and barium polyhydrides  $\text{SrH}_{22}$  [4] and  $\text{BaH}_{12}$  [5], and various rubidium and cesium polyhydrides [6]. Although the stabilization of most polyhydrides currently requires considerable pressures of at least several gigapascals (Table I), the conditions for their stabilization are continuously improving, which gives hope for discovery of alternative stable hydrogen storage compounds with record capacity in the future.

The second promising area of research in hydride chemistry is the designing of high-temperature superconductors with a near-room temperature of superconductivity [7]. At the moment, a well reproducible record superconductor is fcc- $\text{LaH}_{10}$  with a critical superconductivity temperature  $T_C$  of  $250 \pm 5$  K at 150 GPa [8,9]. Superconductivity is distributed unevenly among polyhydrides, being a distinctive feature of mostly cubic and hexagonal hydrides such as  $\text{XH}_6$ ,  $\text{XH}_9$ ,  $\text{XH}_{10}$ , and tetragonal  $\text{XH}_4$  (where  $X = \text{La}, \text{Y}, \text{Sc}, \text{Th}, \text{Ce}, \text{Ca}$ , and some other elements), with the atomic hydrogen

sublattices stabilized at 100–200 GPa [10,11]. In this pressure range, the maximum critical temperatures of the best superhydrides are in the range  $\max T_C [\text{K}] \subset (P, 2P)$  [GPa] (Table S1 in the Supplemental Material [12] (also see [13–17]); see also [18–22]). The hydride-forming element can be sulfur, an alkaline earth metal (Mg, Ca, Sr, Ba), or have only 1–2 *d* or *f* electrons (La, Y, Zr, Th, Ce, Lu, etc.). For all other elements of the periodic table (the “empty” zone), polyhydrides are either not formed or do not exhibit superconducting properties.

In this research, we investigate the Tc-H system, belonging to this “empty” zone, at pressures up to 45 GPa to verify theoretical predictions on the distribution of superconducting properties in polyhydrides [23]. Despite the obvious interest in hydrogen-saturated compounds like  $\text{K}_2\text{TcH}_9$  [23], only a few papers on thermodynamic and quantum mechanical calculations of the Tc-H system for gaseous states of hydrides are found in the literature before 2021 [24–27]. For example, the calculations of the enthalpy of formation of technetium monohydride [28] showed that  $\Delta_f H_m^\circ (\frac{1}{2}\text{TcH}) = +9$  kJ/mole; that is, TcH must decompose spontaneously at ambient pressure and can be stabilized only when pressure is increased.

Experimental works in the synthesis of technetium hydrides at elevated pressures have shown that metallic technetium has a small tendency to react with  $\text{H}_2$  under the ambient temperature and pressure conditions [29]. Spitsyn *et al.* [29] reported the synthesis of  $\text{TcH}_{0.73\pm 0.05}$  via a direct reaction of Tc with hydrogen gas at pressures up to 1.9 GPa and a temperature of 573 K. The resulting hydride formed a single phase with a hexagonal lattice:  $a = 2.805 \pm 0.02$  Å,  $c = 4.455 \pm 0.02$  Å. At an elevated pressure (2.2 GPa), the same team obtained two hexagonal phases with the compositions  $\text{TcH}_{0.5}$  ( $\epsilon_1$ ) and  $\text{TcH}_{0.78}$  ( $\epsilon_2$ ) [30]. The  $\epsilon_1 \rightarrow \epsilon_2$  phase

\*d.zhou@skoltech.ru

†dmitrii.semenov@skoltech.ru

‡guerman\_k@mail.ru

TABLE I. Hydrogen capacity of polyhydrides.

Compound	Stabilization pressure (GPa)	Hydrogen content (wt %)
$[(\text{CH}_4)_3(\text{H}_2)_{25} = \text{CH}_{20.7}]$	10	63
$\text{CH}_4$	0	25
$\text{SrH}_{22}$	80	20
$\text{NH}_3\text{BH}_3$	0	19
$(\text{HI})(\text{H}_2)_{13}$	9	17
$\text{Xe}(\text{H}_2)_8$	5–8	11
$\text{CsH}_{\sim 17}$	10	11
$\text{RbH}_{\sim 9}$	8	9.5
$\text{BaH}_{12}$	75	8

transition, observed at about 1 GPa, was confirmed by resistivity measurements.

The formation of nonstoichiometric hydrides  $\text{TcH}_{0.45}$ ,  $\text{TcH}_{0.69}$  [31,32], and  $\text{TcH}_m$ , where  $m = 0.26$  [33], 0.385, 0.485, and 0.765 [34], was proved using neutron powder diffraction. The hydrides with  $m = 0.45$  and 0.69 have been indexed in the hexagonal space group hcp:  $a = 2.801 \pm 0.004 \text{ \AA}$ ,  $c = 4.454 \pm 0.01 \text{ \AA}$  for  $\text{TcH}_{0.45}$ ;  $a =$

$2.838 \pm 0.004 \text{ \AA}$ ,  $c = 4.465 \pm 0.01 \text{ \AA}$  for  $\text{TcH}_{0.69}$ . Three unexpected peaks in the neutron diffraction patterns have been observed for  $\text{TcH}_{0.45}$  and interpreted as the evidence of a superstructure. The authors concluded that hydrogen atoms occupy octahedral voids in the technetium lattice [31,32].

The studies of the transport properties and superconductivity of the obtained lower hydrides showed that the effect of hydrogen is highly negative to the electron-phonon interaction in technetium. The critical temperature  $T_C$  of the pure metal is about 7.73 K at normal pressure, which is one of the highest values among the pure elements [35]. However,  $\text{TcH}_{0.73 \pm 0.05}$  ( $\epsilon_2$ ) does not have a transition to the superconducting state above 2 K, probably because of the increasing Tc-Tc distance [29,31,36,37].

Theoretical studies of stable compounds in the Tc-H system have been previously conducted using density functional theory (DFT) methods at high and ultrahigh pressures up to 300 GPa [38]. It has been found that increasing pressure leads to the formation of hydrogen-enriched hydrides:  $P6_3/mmc$ -TcH (stable in the range of 0 – 200 GPa),  $I4/mmm$ -TcH<sub>2</sub> (stable above 64 GPa),  $Pnma$ -TcH<sub>3</sub> (stable above 79 GPa), and  $P4_2/mmc$ -TcH<sub>3</sub> (forms at about 300 GPa), in which the charge is partially transferred from the

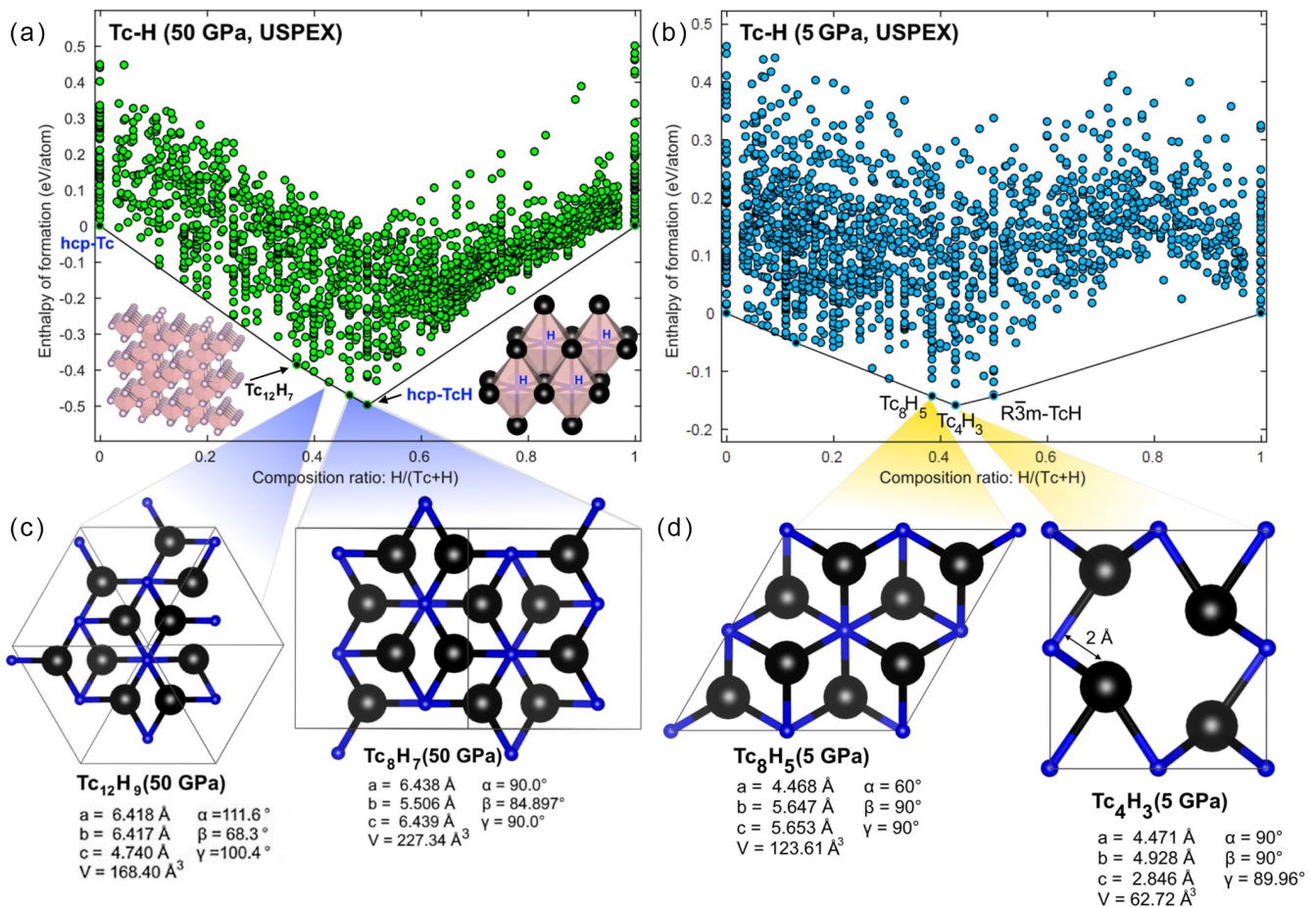


FIG. 1. Calculated convex hulls for the Tc-H system at (a) 50 GPa, (b) 5 GPa, and (c), (d) the most stable crystal structures of pseudo-hexagonal  $\text{TcH}_\gamma$  ( $\gamma = 0.75 \pm 0.12$ ). Inset: (pseudo)hexagonal structures of TcH and  $\text{Tc}_{12}\text{H}_7$ , where hydrogen (H) occupies octahedral voids. Figures were drawn in VESTA [47]. The predicted XRD patterns of these structures and their CIF files are given in the Supplemental Material [12].

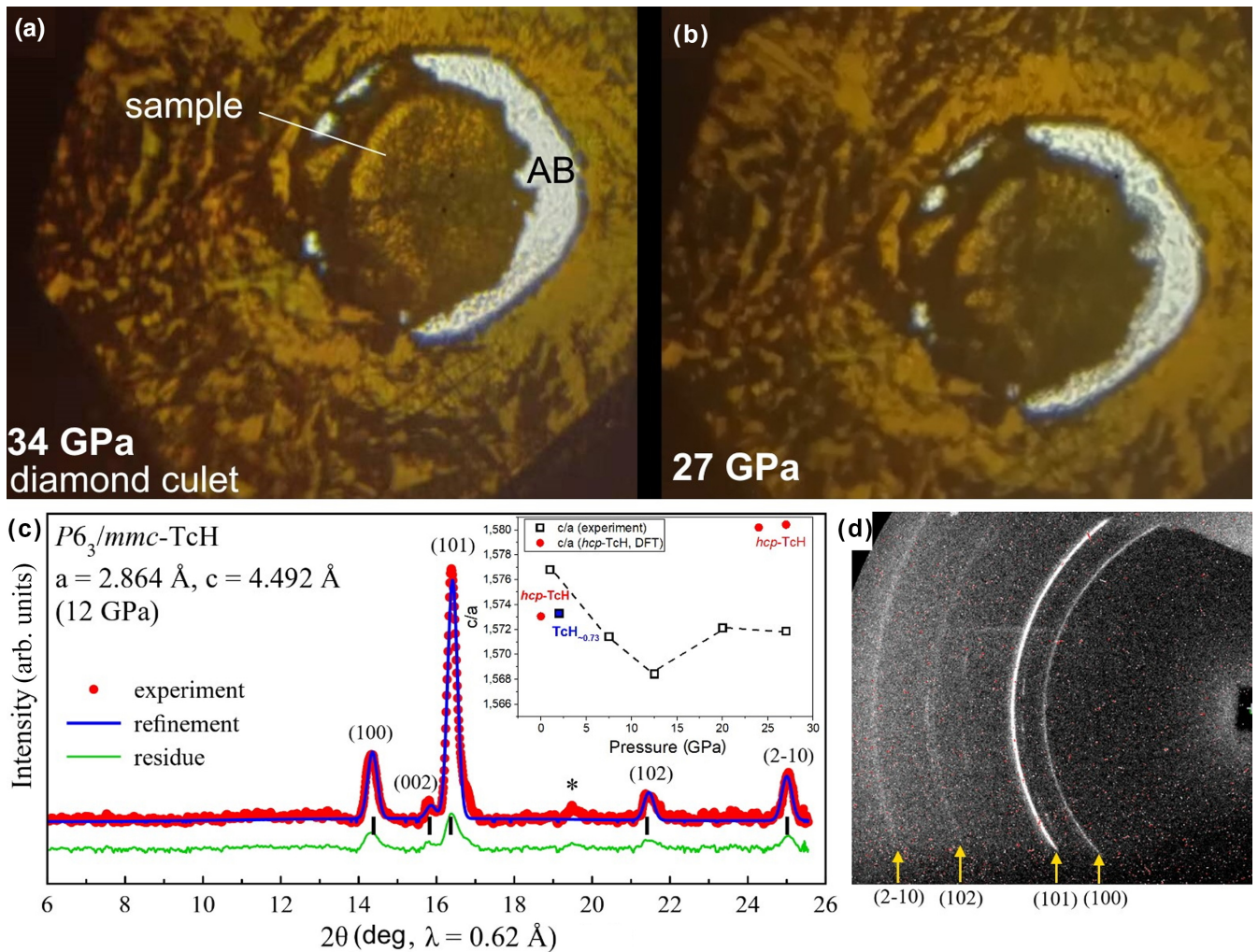


FIG. 2. X-ray powder analysis of technetium hydrides in DAC T1. Microphotographs of the loaded Tc sample (a) before and (b) after the laser heating, where the pressure significantly decreased. (c) Experimental XRD pattern measured at 300 K and the Le Bail refinement of the unit cell parameters of  $P6_3/mmc$ -TcH at 12 GPa. The experimental data, fit, and residue are shown in red, blue, and green, respectively. The unidentified reflections are indicated by asterisks. Inset: Pressure dependence of the  $c/a$  ratio. (d) Experimental diffraction pattern of TcH.

technetium atoms to hydrogen. The theoretically calculated superconducting properties of technetium hydrides are weakly expressed, with  $T_C$  not exceeding 11 K [38].

In this work, we synthesized and characterized technetium hydrides  $\text{TcH}_{1+x}$  ( $x = 0-0.3$ ) at pressures up to 27 GPa using x-ray powder diffraction and at pressures up to 45 GPa using reflection spectroscopy in diamond anvil cells (DACs).

## II. RESULTS AND DISCUSSION

### A. Structure search

At present, theoretical analysis and evolutionary structural search are among the cornerstones in hydride chemistry [39–43] because establishing the exact positions of hydrogen atoms in polyhydrides at high pressures (above 10–20 GPa) is a complex technical task. We performed an evolutionary crystal structure search for thermodynamically stable phases at 5, 25, and 50 GPa in the Tc-H system using the USPEX

code [44–46]. In terms of thermodynamics, the Tc-H system belongs to those where metal-rich phases dominate hydrogen-rich phases (e.g., Sr-H [4], Ba-H [5], etc.).

The calculations resulted in a phase diagram (convex hull, Fig. 1) of technetium hydrides which shows that at 25 GPa (see Supplemental Material, Fig. S1 [12]; see, also, Refs. [13–17] therein) and 50 GPa the highest hydrogen content is achieved in  $P6_3/mmc$ -TcH, whereas all higher hydrides are thermodynamically unstable. Many nonstoichiometric  $\text{TcH}_y$  hydrides ( $y < 1$ ) lie close to the convex hull between Tc and TcH, which speaks in favor of the possible formation of hydrides with intermediate compositions ( $0 < y < 1$ ) at low pressures or hydrogen deficiency. The most stable phases at 50 GPa are pseudo-hexagonal  $P1$ - $\text{Tc}_{12}\text{H}_7$ ,  $P1$ - $\text{Tc}_{12}\text{H}_9$ , and  $P1$ - $\text{Tc}_8\text{H}_7$  (Fig. 1). At 5 GPa, the thermodynamically stable phases are  $\text{Tc}_4\text{H}_3$  and  $\text{Tc}_{16}\text{H}_7$ , which are candidates for previously experimentally found compounds  $\text{TcH}_{0.75\pm 0.05}$  ( $\epsilon_2$ ) and  $\text{TcH}_{0.5\pm 0.05}$  ( $\epsilon_1$ ), respectively.

TABLE II. Experimental unit cell parameters of synthesized technetium hydrides  $\text{TcH}_{1+x}$  ( $x = 0-0.3$ ) and metallic technetium ( $V_{\text{Tc}}$ ) [52].

Pressure (GPa)	$a$ (Å)	$c$ (Å)	$c/a$	$V$ (Å <sup>3</sup> ) ( $Z = 2$ )	$V$ (Å <sup>3</sup> /Tc)	$V_{\text{Tc}}$ (Å <sup>3</sup> /Tc)
27	2.845	4.472	1.572	31.35	15.67	13.28
20	2.849	4.479	1.572	31.49	15.74	13.51
12	2.864	4.492	1.568	31.91	15.95	13.79
7	2.856	4.488	1.571	31.70	15.85	14.00
~1	2.838	4.475	1.572	31.22	15.61	14.30
~2, ( $\text{TcH}_{0.73}$ )	2.838	4.465	1.573	31.14	15.57	14.21
~2, ( $\text{TcH}_{0.45}$ )	2.801	4.454	1.590	30.62	15.31	

### B. Experimental synthesis

Technetium samples mixed with ammonia borane  $\text{NH}_3\text{BH}_3$  were heated in DACs T1 and T2 by a pulsed laser for several hundred microseconds to 1500 K at pressures of 34 GPa (DAC T1, 300  $\mu\text{m}$  culet) and 45 GPa (DAC T2, determined via the Raman signal of diamond [48]). After the laser heating, the pressure in DAC T1 dropped to 27 GPa. Low-pressure x-ray diffraction studies were carried out on a synchrotron source of the Kurchatov Institute (KISI-Kurchatov), station RKFM ( $\lambda = 0.62$  Å, 20 keV; beam width was about 50  $\mu\text{m}$ ).

Figures 2(a) and 2(b) show a substantial change in the character of the technetium surface after the laser heating. As we will see below, the spectral reflectivity of the sample also changes significantly. The XRD analysis [49–51] shows the presence of one hexagonal phase [Fig. 2(c)], whose cell volume at pressures above 10 GPa slightly exceeds the values theoretically calculated for  $P6_3/mmc$ -TcH (Table II), corresponding to compositions  $\text{TcH}_{1.1-1.3}$ . Some XRD patterns also show an hcp admixture of Re (or Tc), which is due to the large width of the x-ray beam ( $\sim 50$   $\mu\text{m}$ ). As the pressure in DAC T1 decreases, so does the hydrogen content in the compound, and at 1–2 GPa the cell parameters of  $\text{TcH}_x$  approach the literature data for the composition  $\text{TcH}_{0.73}$  (Fig. 3) [29,30,34]. This allows us to conclude that stoichiometric TcH is thermodynamically unstable below 10 GPa and loses hydrogen already at 300 K.

The reaction of technetium with hydrogen at high pressures is very similar to the behavior of the Mo-H system, where, also at a pressure of about 15–20 GPa, a nonstoichiometric phase  $\text{MoH}_{1.35}$  forms [53]. However, for example, the behavior of the Re-H system is different: At 20 GPa, only  $\text{ReH}_{0.38}$ , a hydride with substantially lower hydrogen content, is formed [54]. Ruthenium occupies an intermediate position: At 15 GPa, it reacts with hydrogen with the formation of stoichiometric fcc  $\text{RuH}$  [55]. An estimation of the saturation composition of technetium hydride  $\text{TcH}_{1+x}$  ( $x = 0-0.3$ ) at 27 GPa is possible from volumetric considerations. Because the volume expansion per Tc atom is measured using x-ray diffraction, the composition H/Tc of the saturated Tc hydride can be estimated by comparing this volume expansion with the expected volume expansion per H atom. In the hcp structure, the occupation of all octahedral voids by hydrogen leads to TcH stoichiometry. When more hydrogen is used, it is only possible to place all extra hydrogens in the tetrahedral voids. Each hydrogen atom placed in an octahedral interstitial site in a close-packed lattice of technetium expands the lattice by about  $1.86$  Å<sup>3</sup> per H atom, whereas

in a tetrahedral site the volume expansion is  $2.2-3.2$  Å<sup>3</sup> per H atom [56]. Considering that  $\Delta V = V(\text{TcH}_{1+x}) - V(\text{Tc}) = 2.39$  (27 GPa),  $2.23$  (20 GPa),  $2.16$  (12 GPa), and  $1.85$  Å<sup>3</sup>/Tc (7 GPa), we can estimate the maximum hydrogen content of the obtained hydride as  $\text{TcH}_{1.3}$  [Fig. 3(a)], which is quite close to the results of the first-principles calculations.

The strength of the electron-phonon interaction in technetium monohydride TcH was estimated using *ab initio* calculations, which are usually in good agreement with experimental data (e.g., [57]; see also [58–61]). Hydrogen has a negative effect on the superconducting properties of technetium despite the fact that it only slightly directly affects the electronic structure of Tc hydrides, contributing almost nothing to the electron density of states at the Fermi level (Fig. 4(d), Supplemental Material, Figs. S6 and S7 [12]). This is due to the fact that hydrogen occupies the octahedral voids in the hexagonal lattice of technetium, increasing the parameters of the unit cell, which is equivalent to introducing a formally negative pressure to hcp-Tc. This concept is schematically shown in Fig. 3(d). For instance, an extrapolation of the equation of state of Tc (Fig. 3(a), Supplemental Material, Fig. S3 [12]; see also [62,63]) to the negative pressure region shows that the cell volume of the synthesized hydride  $\text{TcH}_{1+x}$  ( $x = 0-0.3$ ) corresponds to a pressure of about  $-30$  GPa. At the same time, the region of negative pressures from 0 to  $-30$  GPa, where the unit cell of Tc is only slightly expanded, is unexplored, and a local increase in the critical temperature  $T_C$  expected there requires either a compression of TcH above 50 GPa, or controlled hydrogenation with a very small amount of  $\text{H}_2$ . From a practical point of view, small levels of hydrogenation with a controlled expansion of the unit cell are achievable using the electrochemical approach [64]. At the same time, as the pressure increases from 0 to 1.5 GPa, the critical temperature of technetium decreases with a slope of  $dT_C/dP = -0.125$  K/GPa [65].

The Crystal orbital Hamilton population (COHP) [66,67] analysis shows (Supplemental Material [12]) that the technetium atoms interact quite strongly with each other (Tc-Tc) and with hydrogen (Tc-H, Figs. S10(c)–10(f) in the Supplemental Material [12]). However, in the vicinity of the Fermi level, the Tc-H interaction is virtually zero, which corresponds to the negligible contribution of the hydrogen sublattice to the conductivity and superconductivity of technetium hydrides. In the hcp-TcH there is a little electronic instability of the Tc-Tc bonds in the vicinity of the Fermi level (Fig. S10(a) in the Supplemental Material [12]), as well as a pronounced contribution of the antibonding orbitals to the H-H interaction

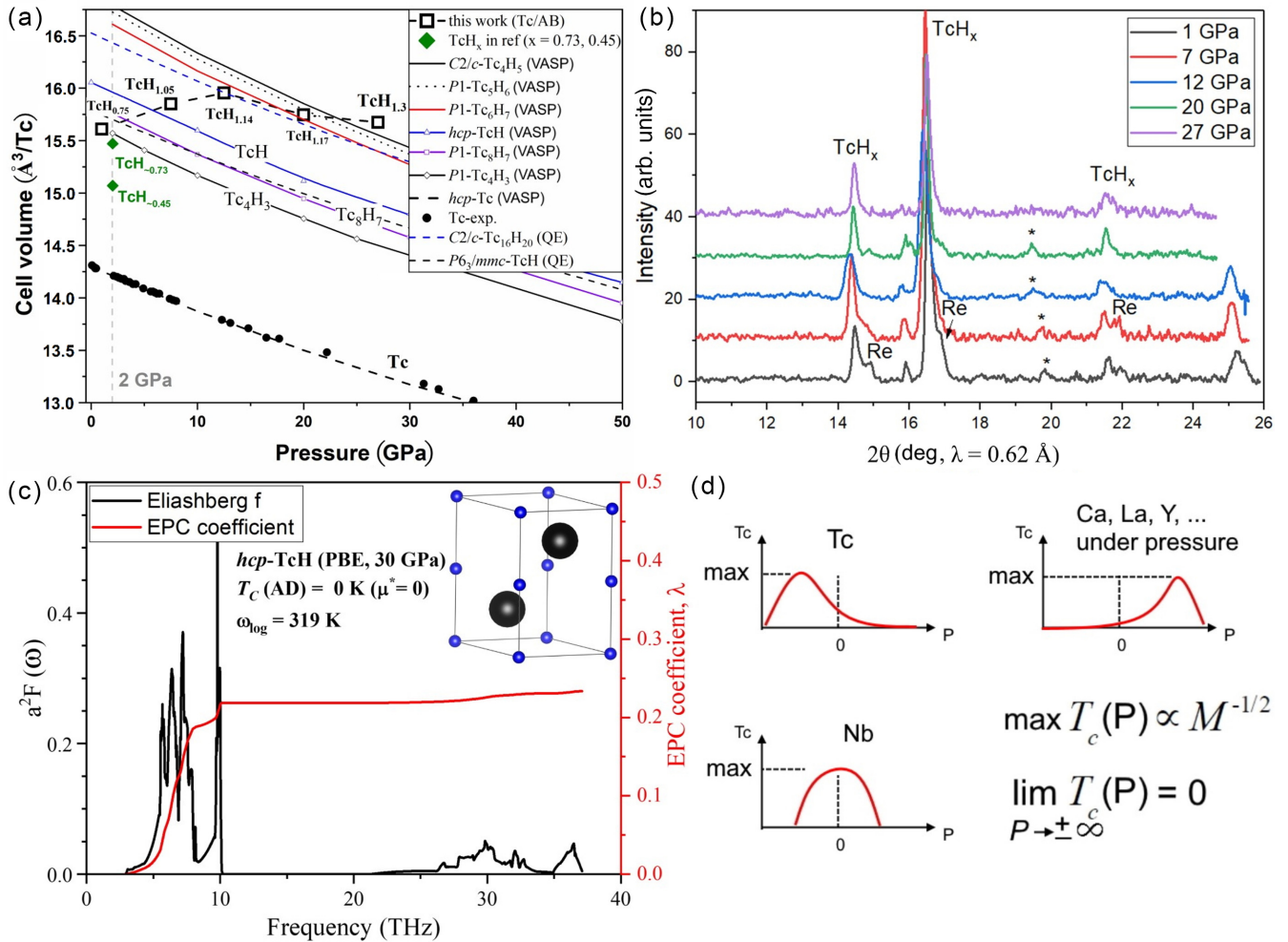


FIG. 3. Physical properties of technetium hydrides. (a) Experimental and theoretical (VASP, QUANTUM ESPRESSO) equations of state of various technetium hydrides and metallic technetium (see also Supplemental Material [12]). (b) X-ray diffraction patterns of the synthesized technetium hydrides during decompression from 27 to  $\sim 1$  GPa. (c) Eliashberg function and the electron-phonon interaction parameter of technetium monohydride  $\text{TcH}$  at 30 GPa. The calculations were performed using the PBE-SP-HGH pseudopotentials in the QUANTUM ESPRESSO code [70,71]. Inset: Crystal structure of hcp-TcH. (d) Schematic representation of different variants of the pressure dependence of the critical temperature of conventional Bardeen-Cooper-Schrieffer superconductivity [72] for metals, where  $M$  is the mass of an atom and  $P$  is the pressure. The maximum critical temperature of Tc can lie both at zero pressure and in the region of a small “negative” pressure.

(Fig. S10(b) in the Supplemental Material [12]). This may indicate that  $\text{TcH}$  will not be stable under decreasing pressure and will lose hydrogen.

According to the *ab initio* calculations [Fig. 3(c)],  $\text{P6}_3/\text{mmc-TcH}$  does not have the superconducting properties because of low electron-phonon interaction ( $\lambda_{\text{SC}} \approx 0.23$  at 30 GPa; method see [68]). The main contribution to the electron-phonon interaction strength ( $\lambda_{\text{SC}}$ ) is made by the acoustic modes of the technetium sublattice. In contrast, pure technetium at normal pressure has high  $\lambda_{\text{SC}} \sim 0.8$  and  $T_C = 7.7 \text{ K}$  [69], possibly due to the proximity of the phase transition which is formally located in the “negative” pressure region. In the region of positive pressures, the hexagonal phase of technetium is stable at least up to 67 GPa [52]. These results are consistent with measurements done in the 1970s–1980s, when it was shown that superconductivity in technetium is suppressed by both excess of hydrogen and external pressure [29,31,36,37].

### C. Reflectance spectroscopy

We investigated the relative reflectance  $R(\lambda)$  of metallic technetium and the synthesized  $\text{TcH}_{1+x}$  ( $x = 0-0.3$ ) hydrides in the high-pressure DAC T2 in the visible spectral region (400–900 nm, 1.4–3.1 eV, Fig. 4). Because the geometry of the diamond anvil, sample, and  $\text{NH}_3\text{BH}_3$  layer is unknown, it is only possible to determine the relative reflectivity of the sample in comparison with the reflection from either the Re gasket or from the empty place such as the diamond/ $\text{NH}_3\text{BH}_3$  boundary (reference) of a diamond anvil [Fig. 4(c)]. Before starting the experiment, a series of calibrations were performed to determine the apparent spectral function of the incandescent lamp after passing the light through the optical system (Supplemental Material [12], Figs. S16–S18). Then, the relative reflectance of the empty diamond cell, rhenium gasket, and copper and tungsten particles in ammonia borane media was measured at ambient pressure (Supplemental

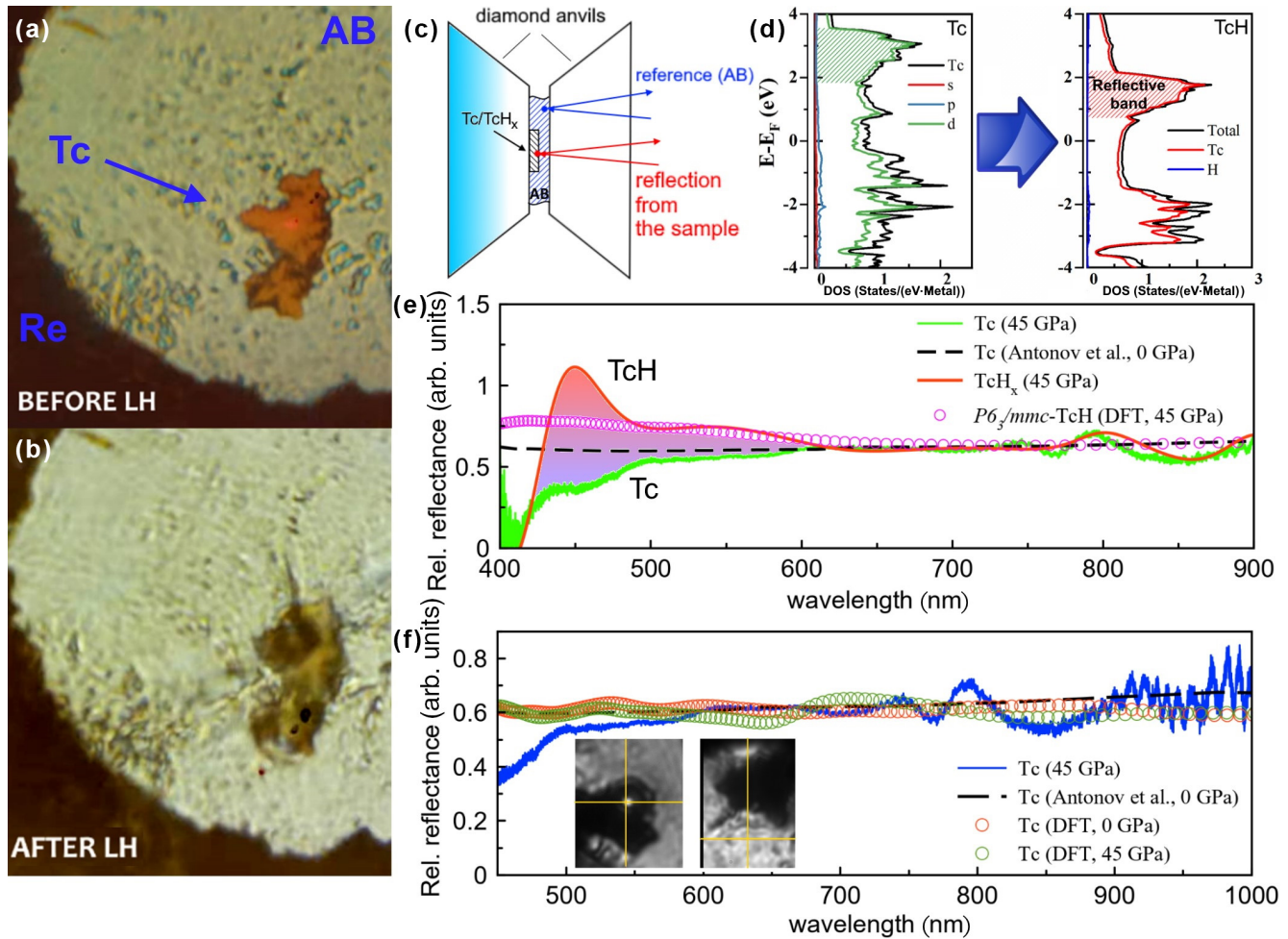


FIG. 4. Reflectance spectroscopy of technetium (Tc) and technetium hydride (TcH) at 45 GPa in DAC T2. Microphotographs of the sample (a) before and (b) after the laser heating at 45 GPa; the pressure was practically unchanged due to the small sample volume (Re is the gasket material, AB is ammonia borane). (c) Schematic of the study of the relative reflectivity  $I_{\text{sample}}/I_{\text{ref}}$ . (d) Changes in the electronic density of states in the reaction  $2\text{Tc} + \text{H}_2 \rightarrow 2\text{TcH}$  at 20 GPa. (e) Smoothed measurement results of the relative reflectivity of Tc (green) and  $\text{TcH}_{1+x}$  (red), calculated data for hcp-TcH (purple) at 45 GPa, and literature data for technetium at 0 GPa (dashed black line). (f) Experimental reflectivity of Tc at 45 GPa (blue) compared with the literature data at 0 GPa (dashed black line) and VASP [77–79] calculation results at 0 (red) and 45 GPa (green).

Material, Figs. S19–S24 [12]). The complex interference pattern was smoothed (using the Fourier filter from OriginLab [73]) and multiplied by an arbitrary normalization constant. The relative reflectance values were calculated as  $R(\lambda) = \text{const} \times I_{\text{sample}}(\lambda)/I_{\text{ref}}(\lambda)$ , where  $I_{\text{sample}}(\lambda)$  and  $I_{\text{ref}}(\lambda)$  are intensities of light reflected from the sample and the reference, respectively. The obtained values agree with the known experimental data for the studied metals (Supplemental Material, Figs. S25–S27 [12]; also see [74]). Reflectance spectra of the compressed sulfur hydride  $\text{H}_3\text{S}$  were recently measured and processed in a similar manner [75,76].

It was found that the accuracy and reproducibility of the reflection spectra do not allow them to be used as an independent method of structure determination even in combination with the DFT calculations of reflectivity. This is primarily due to complex interference patterns and large variations of the reflection spectra in different points of nonuniform powder samples. In addition, calculations of the reflectance require the knowledge of the possible structure of a compound and are

quite time consuming compared to an almost instantaneous prediction using an XRD pattern.

Technetium hydrides are a convenient object for reflection spectroscopy studies. The analysis of the electronic structure of hcp-Tc and hcp-TcH (Fig. 4(d), Supplemental Material, Figs. S6 and S7 [12]) shows that the Fermi level is at a “trough” and is due to the contribution of  $d$  electrons from the Tc atoms; hydrogen makes almost no contribution to the density of states near the Fermi level. When going from technetium to its hydride TcH, we see that the region of high density of unoccupied states shifts closer to the Fermi level [Fig. 4(d)] and transitions with an energy of 2.25–2.5 eV appear near the  $\Gamma$  point (Supplemental Material, Fig. S7 [12]). This is qualitatively consistent with the results of the direct DFT calculations, which also show the emergence of a reflective band in  $R(\lambda)$  at 450–600 nm. This peculiarity of the reflection spectrum is observed in the experiment with technetium hydrides but is absent in the study of pure technetium before the laser heating of the sample [Fig. 4(e)]. After the

laser heating of the Tc/AB sample at 45 GPa, a reflective band (broad peak) appears at 450–600 nm, which can be explained by the presence of hcp- $\text{TcH}_{1+x}$ . At the same time, at 500 – 800 nm, the relative reflectance of Tc agrees with the literature data [80] and results of the DFT calculations [Fig. 4(f)].

### III. CONCLUSIONS

In conclusion, we investigated the formation of lower technetium hydrides at pressures up to 45 GPa using synchrotron x-ray diffraction, reflectance spectroscopy, and first-principles calculations. In the investigated pressure range, the Tc-H system is similar to the Mo-H system: Technetium reacts with hydrogen to form nonstoichiometric hydrides with gradually increasing hydrogen content up to hcp- $\text{TcH}_{1.3}$  at 27 GPa. The formation of technetium hydrides is also confirmed by the emergence of a reflective broad band at 450–600 nm in the hydrogenated Tc samples at 45 GPa. The dependence of the relative reflectance on the wavelength at 450–900 nm for Tc and  $\text{TcH}_{1+x}$  was established. *Ab initio* calculations show that lower technetium hydrides do not possess superconducting properties.

Relatively simple reflectance spectroscopy provides additional evidence of hydride formation in the Tc-H system and can be used independently of synchrotron x-ray diffraction. The developed approach to the reflectance spectra studies can be useful as a complementary method to confirm the structure of polyhydrides synthesized in diamond anvil cells at ultrahigh pressures. These optical measurements do not require the use of cryogenic equipment, sputtering of electrodes, and synchrotron radiation sources, and can be implemented in almost any high-pressure laboratory.

### IV. SUPPORTING INFORMATION

The raw and processed data required to reproduce these findings are available to download from GitHub and as Supplemental Material [12] for the manuscript.

The video of the laser heating of Tc samples can be seen in [81]. The x-ray diffraction data can be found in [82]. The

reflection spectroscopy data can be found in [83]. The results of the structural search are available in [84].

### ACKNOWLEDGMENTS

*In situ* x-ray diffraction experiments at high pressures were performed on a synchrotron source of the Kurchatov Institute (KISI-Kurchatov), station RKFM. The high-pressure experiments were supported by the Ministry of Science and Higher Education of the Russian Federation within the state assignment of the FSRC Crystallography and Photonics of the RAS while the radiochemistry part was carried out in the frame of MSHERF Topic No. AAAA-A18-118040590105-4). I.A.T. was supported by the Russian Science Foundation, Project No. 22-12-00163. A.R.O. thanks the Russian Science Foundation (Grant No. 19-72-30043). D.V.S. thanks the Russian Foundation for Basic Research (Project No. 20-32-90099) and the Russian Science Foundation, Grant No. 22-22-00570. We also thank Dr. Alexander G. Kvashnin (Skoltech) for the help in calculations of dielectric functions.

D.Z., D.V.S., and M.A.V. contributed equally to this work. D.Z., D.V.S., M.A.V., I.A.T., A.Yu.S., and D.A.S. performed the experiments. D.Z. and D.V.S. prepared the diamond anvil cells and studied the samples in them. M.A.V. and K.E.G. prepared metallic technetium for the experiments. I.A.T. carried out the laser heating of the samples in DACs. A.Yu.S. helped with the x-ray diffraction study at the Kurchatov synchrotron source, RKFM station (Moscow). D.Z. and D.V.S. prepared the theoretical analysis and calculated the equation of states, electron and phonon band structures, and superconducting and optical properties of the samples. I.V.C. performed COHP calculations using the LOBSTER code. D.A.S. built a system to study the optical properties of hydrides at high pressures. D.V.S., D.Z., and A.R.O. analyzed and interpreted the experimental results and wrote the manuscript. P.G.L., A.R.O., and K.E.G. directed the research, analyzed the results, and edited the paper. All the authors provided critical feedback and helped shape the research.

The authors declare no competing financial interests.

- 
- [1] N. A. Ali, N. A. Sazelee, and M. Ismail, *Int. J. Hydrog. Energy* **46**, 31674 (2021).
  - [2] U. Ranieri, L. J. Conway, M.-E. Donnelly, H. Hu, M. Wang, P. Dalladay-Simpson, M. Peña-Alvarez, E. Gregoryanz, A. Hermann, and R. T. Howie, *Phys. Rev. Lett.* **128**, 215702 (2022).
  - [3] J. Binns, P. Dalladay-Simpson, M. Wang, G. J. Ackland, E. Gregoryanz, and R. T. Howie, *Phys. Rev. B* **97**, 024111 (2018).
  - [4] D. V. Semenov, W. Chen, X. Huang, D. Zhou, I. A. Kruglov, A. B. Mazitov, M. Galasso, C. Tantarini, X. Gonze, A. G. Kvashnin *et al.*, *Adv. Mater.* **34**, 2200924 (2022).
  - [5] W. Chen, D. V. Semenov, A. G. Kvashnin, X. Huang, I. A. Kruglov, M. Galasso, H. Song, D. Duan, A. F. Goncharov, V. B. Prakapenka *et al.*, *Nat. Commun.* **12**, 273 (2021).
  - [6] D. V. Semenov, Structural and transport studies of compressed ternary polyhydrides (unpublished).
  - [7] I. A. Troyan, D. V. Semenov, A. G. Ivanova, A. G. Kvashnin, D. Zhou, A. V. Sadakov, O. A. Sobolevsky, V. M. Pudalov, and A. R. Oganov, *Phys.-Usp.* **65**, 748 (2022).
  - [8] A. P. Drozdov, P. P. Kong, V. S. Minkov, S. P. Besedin, M. A. Kuzovnikov, S. Mozaffari, L. Balicas, F. F. Balakirev, D. E. Graf, V. B. Prakapenka *et al.*, *Nature (London)* **569**, 528 (2019).
  - [9] M. Somayazulu, M. Ahart, A. K. Mishra, Z. M. Geballe, M. Baldini, Y. Meng, V. V. Struzhkin, and R. J. Hemley, *Phys. Rev. Lett.* **122**, 027001 (2019).
  - [10] F. Peng, Y. Sun, C. J. Pickard, R. J. Needs, Q. Wu, and Y. Ma, *Phys. Rev. Lett.* **119**, 107001 (2017).
  - [11] D. V. Semenov, I. A. Kruglov, I. A. Savkin, A. G. Kvashnin, and A. R. Oganov, *Curr. Opin. Solid State Mater. Sci.* **24**, 100808 (2020).

- [12] See Supplemental Material at <http://link.aps.org/supplemental/10.1103/PhysRevB.107.064102> for methods, crystal structures, convex hulls, theoretical calculations, Raman spectroscopy, and reflectance spectroscopy. Also see Refs. [13–17].
- [13] P. Hohenberg and W. Kohn, *Phys. Rev.* **136**, B864 (1964).
- [14] W. Kohn and L. J. Sham, *Phys. Rev.* **140**, A1133 (1965).
- [15] J. P. Perdew, K. Burke, and M. Ernzerhof, *Phys. Rev. Lett.* **77**, 3865 (1996).
- [16] G. Kresse and D. Joubert, *Phys. Rev. B* **59**, 1758 (1999).
- [17] P. E. Blöchl, *Phys. Rev. B* **50**, 17953 (1994).
- [18] A. P. Drozdov, M. I. Eremets, I. A. Troyan, V. Ksenofontov, and S. I. Shylin, *Nature (London)* **525**, 73 (2015).
- [19] P. Kong, V. S. Minkov, M. A. Kuzovnikov, A. P. Drozdov, S. P. Besedin, S. Mozaffari, L. Balicas, F. F. Balakirev, V. B. Prakapenka, S. Chariton *et al.*, *Nat. Commun.* **12**, 5075 (2021).
- [20] D. V. Semenov, A. G. Kvashnin, A. G. Ivanova, V. Svitlyk, V. Y. Fominski, A. V. Sadakov, O. A. Sobolevskiy, V. M. Pudalov, I. A. Troyan, and A. R. Oganov, *Mater. Today* **33** (March), 36 (2020).
- [21] W. Chen, D. V. Semenov, X. Huang, H. Shu, X. Li, D. Duan, T. Cui, and A. R. Oganov, *Phys. Rev. Lett.* **127**, 117001 (2021).
- [22] L. Ma, K. Wang, Y. Xie, X. Yang, Y. Wang, M. Zhou, H. Liu, X. Yu, Y. Zhao, H. Wang *et al.*, *Phys. Rev. Lett.* **128**, 167001 (2022).
- [23] A. P. Ginsberg, *Inorg. Chem.* **3**, 567 (1964).
- [24] V. S. Mastryukov, *J. Struct. Chem.* **13**, 539 (1972).
- [25] S. R. Langhoff, L. G. M. Pettersson, C. W. Bauschlicher, and H. Partridge, *J. Chem. Phys.* **86**, 268 (1987).
- [26] J.-Z. Wang and K. Balasubramanian, *J. Mol. Spectrosc.* **138**, 204 (1989).
- [27] K. Balasubramanian and J. Z. Wang, *J. Chem. Phys.* **91**, 7761 (1989).
- [28] P. C. P. Bouten and A. R. Miedema, *J. Less-Common Met.* **71**, 147 (1980).
- [29] V. I. Spitsyn, E. G. Ponyatovskii, V. E. Antonov, I. T. Belash, and O. A. Balakhovskii, *Proc. Acad. Sci. USSR* **247**, 1420 (1979).
- [30] V. I. Spitsyn, V. E. Antonov, O. A. Balakhovskii, I. T. Belash, E. G. Ponyatovskii, V. I. Rashchupkin, and V. S. Shekhtman, *Proc. Acad. Sci. USSR* **260**, 795 (1981).
- [31] V. P. Glazkov, A. V. Irodova, V. A. Somenkov, S. S. Shil'shtejn, V. E. Antonov, and E. G. Ponyatovskij, *Fiz. Tverd. Tela (Leningrad)* **26**, 3261 (1984).
- [32] S. S. Shilstein, V. P. Glazkov, A. V. Irodova, V. A. Somenkov, V. E. Antonov, and E. G. Ponyatovskii, *Z. Phys. Chem. (Munich)* **146**, 129 (1985).
- [33] E. N. Zakharov, S. P. Bagaev, V. N. Kudryavtsev, K. S. Pedan, and V. E. Antonov, *Prot. Met. (Engl. Transl.)* **27**, 795 (1992).
- [34] V. E. Antonov, I. T. Belash, K. G. Bukov, O. V. Zharikov, A. V. Pal'nichenko, and V. M. Teplinskij, *Phys. Met. Metallogr.* **68**, 153 (1989).
- [35] S. T. Sekula, R. H. Kernohan, and G. R. Love, *Phys. Rev.* **155**, 364 (1967).
- [36] V. I. Spitsyn, V. E. Antonov, O. A. Balakhovskij, I. T. Belash, E. G. Ponyatovskij, V. I. Rashchupkin, and V. S. Shekhtman, *Dokl. Akad. Nauk SSSR* **260**, 132 (1981).
- [37] V. E. Antonov, *J. Alloys Compd.* **330**, 110 (2002).
- [38] X. Li, H. Liu, and F. Peng, *Phys. Chem. Chem. Phys.* **18**, 28791 (2016).
- [39] D. Zhou, D. V. Semenov, D. Duan, H. Xie, X. Huang, W. Chen, X. Li, B. Liu, A. R. Oganov, and T. Cui, *Sci. Adv.* **6**, eaax6849 (2020).
- [40] D. Zhou, D. V. Semenov, H. Xie, A. I. Kartsev, A. G. Kvashnin, X. Huang, D. Duan, A. R. Oganov, and T. Cui, *J. Am. Chem. Soc.* **142**, 2803 (2020).
- [41] D. V. Semenov, D. Zhou, A. G. Kvashnin, X. Huang, M. Galasso, I. A. Kruglov, A. G. Ivanova, A. G. Gavriluk, W. Chen, N. V. Tkachenko *et al.*, *J. Phys. Chem. Lett.* **12**, 32 (2021).
- [42] I. A. Troyan, D. V. Semenov, A. G. Kvashnin, A. V. Sadakov, O. A. Sobolevskiy, V. M. Pudalov, A. G. Ivanova, V. B. Prakapenka, E. Greenberg, A. G. Gavriluk *et al.*, *Adv. Mater.* **33**, 2006832 (2021).
- [43] D. V. Semenov, I. A. Troyan, A. G. Kvashnin, A. G. Ivanova, M. Hanfland, A. V. Sadakov, O. A. Sobolevskiy, K. S. Pervakov, A. G. Gavriluk, I. S. Lyubutin *et al.*, *Mater. Today* **48** (Sept.), 18 (2021).
- [44] A. R. Oganov, R. O. Lyakhov, and M. Valle, *Acc. Chem. Res.* **44**, 227 (2011).
- [45] A. R. Oganov and C. W. Glass, *J. Chem. Phys.* **124**, 244704 (2006).
- [46] A. O. Lyakhov, A. R. Oganov, H. T. Stokes, and Q. Zhu, *Comput. Phys. Commun.* **184**, 1172 (2013).
- [47] K. Momma and F. Izumi, *J. Appl. Crystallogr.* **44**, 1272 (2011).
- [48] M. I. Eremets, *J. Raman Spectrosc.* **34**, 515 (2003).
- [49] C. Prescher and V. B. Prakapenka, *High Pressure Res.* **35**, 223 (2015).
- [50] V. Petříček, M. Dušek, and L. Palatinus, *Z. Kristallogr.* **229**, 345 (2014).
- [51] A. Le-Bail, *Powder Diffr.* **20**, 316 (2005).
- [52] D. S. Mast, E. Kim, E. M. Siska, F. Poineau, K. R. Czerwinski, B. Lavina, and P. M. Forster, *J. Phys. Chem. Solids* **95**, 6 (2016).
- [53] M. A. Kuzovnikov, H. Meng, and M. Tkacz, *J. Alloys Compd.* **694**, 51 (2017).
- [54] T. Atou and J. V. Badding, *J. Solid State Chem.* **118**, 299 (1995).
- [55] M. A. Kuzovnikov and M. Tkacz, *Phys. Rev. B* **93**, 064103 (2016).
- [56] Y. Fukai, *The Metal-Hydrogen System*, 2nd ed., Springer Series in Materials Science Vol. 21 (Springer-Verlag, Berlin, 2005).
- [57] S. Saib, H. Y. Uzunok, E. R. Karaca, S. Bağcı, H. M. Tütüncü, and G. P. Srivastava, *J. Appl. Phys.* **130**, 153902 (2021).
- [58] A. Togo and I. Tanaka, *Scr. Mater.* **108**, 1 (2015).
- [59] A. Togo, F. Oba, and I. Tanaka, *Phys. Rev. B* **78**, 134106 (2008).
- [60] S. Baroni, S. D. Gironcoli, A. D. Corso, and P. Giannozzi, *Rev. Mod. Phys.* **73**, 515 (2001).
- [61] M. Kawamura, Y. Gohda, and S. Tsuneyuki, *Phys. Rev. B* **89**, 094515 (2014).
- [62] S. Goedecker, M. Teter, and J. Hutter, *Phys. Rev. B* **54**, 1703 (1996).
- [63] C. Hartwigsen, S. Goedecker, and J. Hutter, *Phys. Rev. B* **58**, 3641 (1998).
- [64] E. Piatti, G. Prando, M. Meinero, C. Tresca, M. Putti, S. Roddaro, G. Lamura, T. Shiroka, P. Carretta, and G. Profeta, *arXiv:2205.12951*.

- [65] C. W. Chu, W. E. Gardner, and T. F. Smith, *Phys. Lett. A* **26**, 627 (1968).
- [66] R. Dronskowski and P. E. Bloechl, *J. Phys. Chem.* **97**, 8617 (1993).
- [67] S. Maintz, V. L. Deringer, A. L. Tchougréeff, and R. Dronskowski, *J. Comput. Chem.* **37**, 1030 (2016).
- [68] P. B. Allen and R. C. Dynes, *Phys. Rev. B* **12**, 905 (1975).
- [69] A. K. Shah, R. Khatiwada, N. P. Adhikari, and R. P. Adhikari, *Solid State Commun.* **340**, 114526 (2021).
- [70] P. Giannozzi, S. Baroni, N. Bonini, M. Calandra, R. Car, C. Cavazzoni, D. Ceresoli, G. L. Chiarotti, M. Cococcioni, I. Dabo *et al.*, *J. Phys.: Condens. Matter* **21**, 395502 (2009).
- [71] P. Giannozzi, O. Andreussi, T. Brumme, O. Bunau, M. Buongiorno Nardelli, M. Calandra, R. Car, C. Cavazzoni, D. Ceresoli, M. Cococcioni *et al.*, *J. Phys.: Condens. Matter* **29**, 465901 (2017).
- [72] J. Bardeen, L. N. Cooper, and J. R. Schrieffer, *Phys. Rev.* **108**, 1175 (1957).
- [73] OriginPro. (OriginLab Corporation, Northampton, MA, USA, 2021).
- [74] S. Adachi, *The Handbook on Optical Constants of Metals: In Tables and Figures* (World Scientific Publishing Co., Singapore, 2012).
- [75] F. Capitani, B. Langerome, J. B. Brubach, P. Roy, A. Drozdov, M. I. Eremets, E. J. Nicol, J. P. Carbotte, and T. Timusk, *Nat. Phys.* **13**, 859 (2017).
- [76] P. Roy, J. B. Brubach, F. Capitani, B. Langerome, A. Drozdov, M. I. Eremets, E. J. Nicol, and T. Timusk, *Nat. Phys.* **18**, 1036 (2022).
- [77] G. Kresse and J. Furthmüller, *Phys. Rev. B* **54**, 11169 (1996).
- [78] G. Kresse and J. Hafner, *Phys. Rev. B* **49**, 14251 (1994).
- [79] G. Kresse and J. Hafner, *Phys. Rev. B* **47**, 558 (1993).
- [80] V. N. Antonov, M. M. Kirillova, E. E. Krasovskij, and Y. S. Ponosov, *J. Exp. Theor. Phys.* **94**, 192 (1988).
- [81] <https://youtube.com/shorts/c-TePaqiEkw>.
- [82] <https://github.com/mark6871/technetium-hydrides/tree/XRD>.
- [83] <https://github.com/mark6871/technetium-hydrides/tree/Reflection-spectroscopy>.
- [84] <https://github.com/mark6871/technetium-hydrides/tree/USPEX>.